Coulomb explosions and energy loss of molecular ions in plasmas

Gui-Qiu Wang* and You-Nian Wang
The State Key Laboratory of Materials Modification, Department of Physics, Dalian University of Technology, Dalian 116023, People's Republic of China

Z. L. Mišković
Department of Applied Mathematics, University of Waterloo, Waterloo, Ontario, Canada N2L 3G1
(Received 28 May 2003; revised manuscript received 8 July 2003; published 29 September 2003)

Interactions of swift molecular ions with high-density plasma targets are studied by means of the linearized Vlasov-Poisson theory, allowing the dynamically screened interaction potential among the constituent ions to be expressed in terms of the classical plasma dielectric function. Coulomb explosions and the energy losses of a molecular ion are simulated by solving the equations of motion for the constituent ions. It is found that, due to the wakelike asymmetry of the interaction potential, the molecular axis tends to align itself along the beam direction. In addition, a strong enhancement of the energy loss of the molecular ion has been found in the initial stages of Coulomb explosions due to proximity of the constituent ions, but this effect diminishes at latter stages when the ions are sufficiently far apart.

DOI: 10.1103/PhysRevE.68.036405 PACS number(s): 52.40.Mj, 34.50.Bw, 61.85.+p, 34.50.Dy

I. INTRODUCTION

The problem of interactions of fast ion beams with matter has been the subject of increasing interest during the past several decades, due to its importance in material surface modifications and in the inertial confinement fusion (ICF) [1]. In particular, there exists a promising ICF scheme to drive a *DT* plasma target towards the ignition conditions by using ion-cluster beams, taking advantage of the requirements for lower beam current, weaker beam focusing, and a smaller range for such beams.

The energy loss of ion beams in plasmas is an important quantity for the ICF. For atomic ions moving in plasmas, the energy loss is well understood based on various theoretical models, such as the linear Vlasov-Poisson theory [2–5], the binary collision theory [6], and the nonlinear Vlasov-Poisson theory [7,8]. For the slowing-down processes of ion clusters or molecular ions in plasmas, however, it has been shown that the energy loss of an ion cluster is strongly influenced by the interference resulting from spatial correlation among the cluster constituent particles. This so-called vicinage effect on the energy loss of ion clusters in plasma targets has been described theoretically by several authors [9–17] within the framework of the linearized Vlasov-Poisson theory.

Since the constituent atoms of a cluster are efficiently stripped of their electrons soon upon entering a target, the cluster experiences Coulomb explosion which influences the energy loss processes in the course of cluster penetration through the target. For example, in solid targets, it has been shown [18–20] that the Coulomb explosion patterns of clusters exhibit strong asymmetries for prolonged penetration times, owing to the wake effects in the dynamic response of the target electrons. In particular, a self-consistent model [21,22] was developed recently to study the influence of ion charge states and Coulomb explosions on energy losses of swift molecular ions penetrating through solids. On the other hand, for plasma targets Bret and Deutsch [23] have performed an analytical study, supplemented by a molecular-dynamics (MD) simulation, of Coulomb explosions of fast clusters moving in a hot plasma, modeling the interionic interaction potential by a radially symmetric Debye screening which does not include the wake effects.

To the best of our knowledge, there were no studies reported on the cluster energy losses in plasmas in the presence of Coulomb explosions including the wake effects. We therefore present in this paper self-consistent calculations of Coulomb explosions and energy losses of a molecular ion in a plasma target. In Sec. II, we use the linearized Vlasov-Poisson equations to derive general expressions for the dynamically screened interaction potential and the corresponding force among the constituent ions of a cluster in a plasma target. Next, we simulate in Sec. III the Coulomb explosion dynamics of the cluster by solving the equations of motion for the constituent ions. The energy loss of a cluster undergoing Coulomb explosion is evaluated in Sec. IV as a function of the penetration time through the target. A brief summary of the results is presented in Sec. V.

II. INTERACTION POTENTIAL

Let us first consider a point ion with the charge number Z_1 which moves at the velocity $\mathbf{v}_p$ through a plasma target, characterized by the density n_0 and the electron temperature T_e. The charge density of the projectile is

$$\rho_{ext}(\mathbf{r},t) = Z_1 e\,\delta(\mathbf{r}-\mathbf{v}_p t). \tag{1}$$

Assuming that the projectile velocity is far greater than the ion thermal velocity in the plasma, it follows that only the contributions from the electron component of the plasma will be relevant in the following. The total scalar potential $\Phi(\mathbf{r},t)$ in plasma due to the presence of the ion can be determined from the linearized Vlasov-Poisson equations

*Electronic address: wang_gui_qiu@yahoo.com.cn

$$\left(\frac{\partial}{\partial t}+\mathbf{v}\cdot\frac{\partial}{\partial \mathbf{r}}\right)f_1(\mathbf{r},\mathbf{v},t)=-\frac{e}{m_e}\frac{\partial\Phi}{\partial\mathbf{r}}\cdot\frac{\partial f_0(\mathbf{v})}{\partial\mathbf{v}}, \quad (2)$$

$$\nabla^2\Phi(\mathbf{r},t)=4\pi\left[e\int d\mathbf{v}f_1(\mathbf{r},\mathbf{v},t)-\rho_{ext}(\mathbf{r},t)\right], \quad (3)$$

where m_e is the electron mass, f_1 is the perturbed electron distribution function, and f_0 is the unperturbed electron distribution function which is taken to be Maxwellian. Upon solving Eqs. (2) and (3) by means of the space-time Fourier transform, we obtain

$$\Phi(\mathbf{r},t)=\frac{Z_1e}{2\pi^2}\int\frac{d^3k}{k^2}\frac{1}{\varepsilon(k,\mathbf{k}\cdot\mathbf{v}_p)}\exp[i\mathbf{k}\cdot(\mathbf{r}-\mathbf{v}_pt)], \quad (4)$$

showing that the potential $\Phi(\mathbf{r},t)$ is stationary in the frame of reference moving with the ion. In Eq. (4), $\varepsilon(k,\omega)$ is the longitudinal dielectric function of the classical electron plasma,

$$\varepsilon(k,\omega)=1+(k\lambda_D)^{-2}[X(\omega/kv_T)+iY(\omega/kv_T)], \quad (5)$$

with

$$X(\varsigma)=1-2\varsigma e^{-\varsigma^2}\int_0^{\varsigma}e^{t^2}dt,$$

$$Y(\varsigma)=\sqrt{\pi}\varsigma e^{-\varsigma^2},$$

$v_T=\sqrt{T_e/m_e}$ being the electron thermal speed and $\lambda_D=(T_e/4\pi e^2n_0)^{1/2}$ being the electron Debye screening length.

Next, consider a fast homonuclear diatomic molecular ion moving in the plasma. The interaction potential between the two constituent ions, located at $\mathbf{r}_1$ and $\mathbf{r}_2$ in the center of mass frame of the moving molecular ion, is independent of time and is expressed as

$$U(\mathbf{r}_{12})=\int d\mathbf{r}'\rho_{ext}(\mathbf{r}'-\mathbf{r}_{12},t)\Phi(\mathbf{r}',t)$$

$$=\frac{(Z_1e)^2}{2\pi^2}\int\frac{d^3k}{k^2}\frac{1}{\varepsilon(k,\mathbf{k}\cdot\mathbf{v}_p)}e^{i\mathbf{k}\cdot\mathbf{r}_{12}}, \quad (6)$$

where $\mathbf{r}_{12}=\mathbf{r}_1-\mathbf{r}_2$ is the position of ion 1 relative to ion 2. Assuming that the projectile velocity is directed along the z axis, the potential can be written in cylindrical coordinates $\mathbf{r}_{12}=\{\rho,z,\phi\}$ as follows

$$U(\rho,z)=\frac{2(Z_1e)^2}{\pi v}\int_0^{k_{\max}}\frac{dk}{k}\int_0^{kv_p}d\omega J_0(\rho\sqrt{k^2-\omega^2/v_p^2})$$

$$\times\left\{\cos\left(\frac{\omega z}{v_p}\right)\mathrm{Re}\left[\frac{1}{\varepsilon(k,\omega)}\right]-\sin\left(\frac{\omega z}{v_p}\right)\mathrm{Im}\left[\frac{1}{\varepsilon(k,\omega)}\right]\right\}, \quad (7)$$

where $r_{12}=\sqrt{\rho^2+z^2}$ and $J_0(x)$ is the zeroth-order Bessel function. We have introduced in Eq. (7) a cutoff wave number $k_{\max}=m_e(v_p^2+2v_T^2)/(Z_1e)^2$ to avoid divergence of the integral caused by inadequacy of the classical treatment of the short-range interactions between the projectile and the electrons in plasma [11]. Actually, the k-integral in Eq. (7) is quite insensitive to k_{max}, as long as the internuclear distance r_{12} remains finite and k_{max} is sufficiently large. However, it will be shown in Sec. IV that the influence of k_{max} on the energy loss of individual ions is quite prominent.

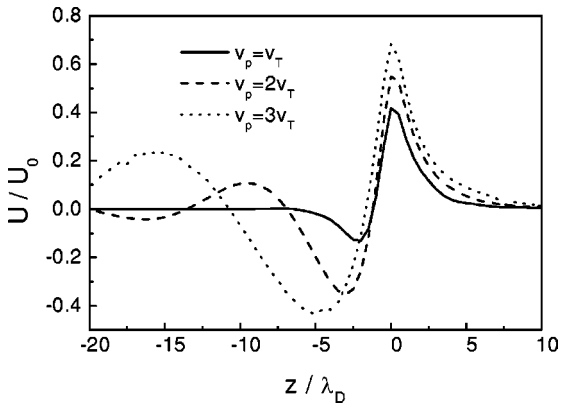

FIG. 1. Total interaction potential U as a function of the longitudinal distance z/λ_D for a two-ion cluster with velocities $v_p=v_T$, $2v_T$, and $3v_T$, moving at the transversal distance $\rho=\lambda_D$ through a plasma with $n_0=10^{20}$ cm^{-3} and $T_e=10^2$ eV. Here, $U_0=(Z_1e)^2/\lambda_D$.

In order to simplify the notation, we introduce dimensionless variables $\tau=k\lambda_D$ and $\varsigma=\omega/kv_T$, so that the interaction potential is finally expressed as

$$U(\rho,z)=U_C(\rho,z)+U_P(\rho,z), \quad (8)$$

where $U_C(\rho,z)=(Z_1e)^2/r_{12}$ is bare Coulomb interaction potential and $U_P(\rho,z)$ is the polarization part of the interaction potential,

$$U_P(\rho,z)=\frac{2(Z_1e)^2}{\pi\lambda_D}\frac{v_T}{v_p}\int_0^{\tau_{\max}}d\tau\int_0^{v_p/v_T}d\varsigma J_0(\rho\tau$$

$$\times\sqrt{1-(v_T\varsigma/v_p)^2})\left[\cos\left(\frac{v_Tz}{v_p\lambda_D}\tau\varsigma\right)G_r(\tau,\varsigma)\right.$$

$$\left.-\sin\left(\frac{v_Tz}{v_p\lambda_D}\tau\varsigma\right)G_i(\tau,\varsigma)\right], \quad (9)$$

with

$$G_r(\tau,\varsigma)=\frac{X(\varsigma)[\tau^2+X(\varsigma)]-Y^2(\varsigma)}{[\tau^2+X(\varsigma)]^2+Y^2(\varsigma)},$$

$$G_i(\tau,\varsigma)=-\frac{\tau^2Y(\varsigma)}{[\tau^2+X(\varsigma)]^2+Y^2(\varsigma)},$$

and $\tau_{\max}=k_{\max}\lambda_D$.

Figure 1 shows the dependence of the total interaction potential U on the longitudinal distance z/λ_D at fixed radial distance $\rho=\lambda_D$, for a molecular ion moving with different

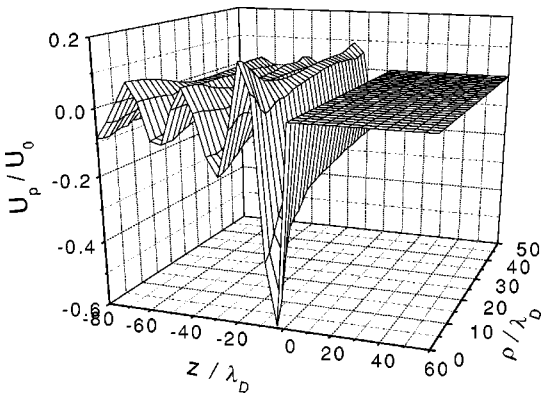

FIG. 2. Polarization part U_p of the interaction potential as a function of the longitudinal distance z/λ_D and the transversal distance ρ/λ_D for a two-ion cluster with the velocity $v_p=2v_T$, moving through a plasma with $n_0=10^{20}$ cm^{-3} and $T_e=10^2$ eV. Here, $U_0=(Z_1e)^2/\lambda_D$.

speeds v_p through a plasma with $n_0=10^{20}$ cm^{-3} and $T_e=10^2$ eV. One observes that the dependence of the potential on the coordinate z is rather asymmetric, as a consequence of the wakelike oscillatory spatial pattern of the medium response. In particular, the wavelength of the oscillations behind the projectile appears to be of the order of $2\pi v_p/\omega_p$, where $w_p=v_T/\lambda_D$ is the electron plasma frequency, in analogy to the wakes in solid targets [24]. In order to further reveal the characteristics of the wake effects, we plot in Fig. 2 the dependence of the polarization part of the potential on both ρ/λ_D and z/λ_D for a projectile velocity $v_p=2v_T$, in the plasma with the same parameters as in Fig. 1.

III. COULOMB EXPLOSIONS

During penetration through a plasma, a molecular ion dissociates into a cluster composed of two ions. The Coulomb explosion patterns can be described by solving the equations of motion for the individual ions within the cluster. Thus, for the jth ion, one has

$$m\frac{d^2\mathbf{r}_j}{dt^2}=\mathbf{F}_j^s+\sum_{l\neq j=1}^{2}\mathbf{F}(\mathbf{r}_{jl}), \tag{10}$$

where m is the ion mass, $\mathbf{F}_j^s=-\partial U(\mathbf{r}_{jl})/\partial\mathbf{r}_{jl}|_{\mathbf{r}_{jl}=0}$ is the self-stopping force, while the interaction force is given by $\mathbf{F}(\mathbf{r}_{jl})=-\partial U(\mathbf{r}_{jl})/\partial\mathbf{r}_{jl}$, for $j\neq l$.

Since the velocities $\mathbf{v}_j$ of the individual ions change only slightly during the passage, we may retain the initial velocity $\mathbf{v}_p$ in those expressions of the preceding section which are used to evaluate the forces in Eq. (10). Thus, the self-stopping force acts in the direction of motion and depends on the speed v_p, i.e., $\mathbf{F}_1^s=\mathbf{F}_2^s=F_s(v_p)\hat{\mathbf{e}}_z$. Using the interaction potential (9), the stopping force can be expressed as

$$F_s(v_p)=-\frac{2(Z_1e)^2}{\pi\lambda_D^2}\left(\frac{v_T}{v_p}\right)^2\int_0^{v_0/v_T}\varsigma Y(\varsigma)I(\varsigma,\tau_{\max})d\varsigma, \tag{11}$$

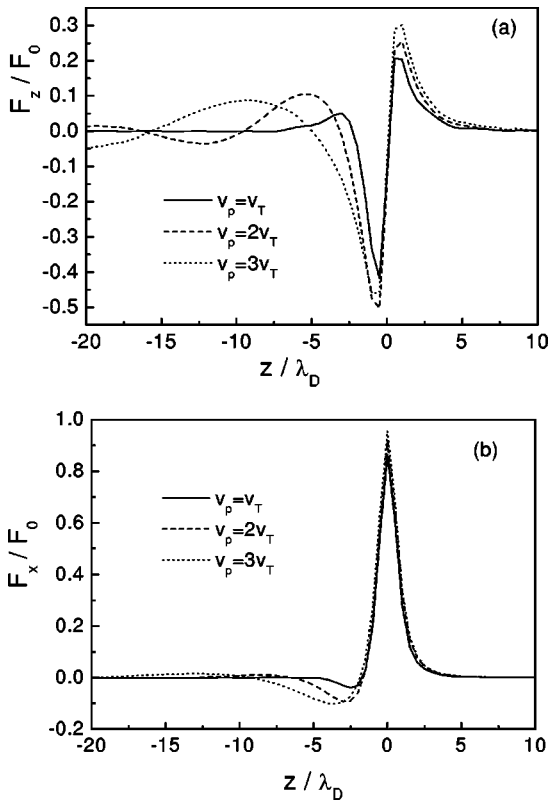

FIG. 3. The dependence of (a) the longitudinal, F_z, and (b) the transversal, F_x, component of the total interaction force on the longitudinal distance z/λ_D for a two-ion cluster with velocities $v_p=v_T$, $2v_T$, and $3v_T$, moving at the transversal distance $\rho=\lambda_D$ through a plasma with $n_0=10^{20}$ cm^{-3} and $T_e=10^2$ eV. Here, $F_0=(Z_1e)^2/\lambda_D^2$.

where

$$I(\varsigma,\tau_{\max})=\frac{1}{4}\ln\left[\frac{(\tau_{\max}^2+X(\varsigma))^2}{X^2(\varsigma)+Y^2(\varsigma)}\right]-\frac{X(\varsigma)}{2Y(\varsigma)}\times\left[\tan^{-1}\left(\frac{\tau_{\max}^2+X(\varsigma)}{Y(\varsigma)}\right)-\tan^{-1}\left(\frac{X(\varsigma)}{Y(\varsigma)}\right)\right],$$

which exhibits a rather strong influence of $\tau_{max}=k_{max}\lambda_D$.

In analogy to the interaction potential (8), the interaction force $\mathbf{F}$ can be also decomposed into two parts, i.e., $\mathbf{F}=\mathbf{F}^C+\mathbf{F}^P$, where $\mathbf{F}^C$ is bare Coulomb force and $\mathbf{F}^P$ is the polarization part of the interaction force. Figures 3(a) and 3(b) show, respectively, the dependences of the longitudinal, F_z, and the transversal, F_x, components of the total interaction force between the two ions on the longitudinal distance z/λ_D, with fixed transversal distance $\rho=\lambda_D$, for the same set of parameters as in Fig. 1.

It is convenient to study the Coulomb explosion dynamics of a diatomic molecule in terms of the relative position $\mathbf{r}=\mathbf{r}_1-\mathbf{r}_2$ and the relative velocity $\mathbf{u}=\mathbf{v}_1-\mathbf{v}_2$. Since we want to explore a wide range of plasma parameters, it is instructive to introduce the logarithm of the dimensionless time variable $\xi=\log_{10}(t/t_c)$, where for the characteristic time we choose $t_c=\sqrt{mr_0^3/(4Z_1^2e^2)}$, characterizing an explosion in

bare Coulomb field, with r_0 being the initial internuclear distance. Note that t_c can be defined by $t_c = r_0/u_c$, where u_c is the relative radial speed of the constituent ions after long time, obtained from the conservation of energy in bare Coulomb potential, $\frac{1}{2}(m/2)u_c^2 = ((Z_1 e)^2)/r_0$. Using the chain rule $d/dt = (d\xi/dt)d/d\xi = (1/\alpha(\xi)t_c)(d/d\xi)$ to change the variable t to ξ in Eqs. (10), we obtain the following equations for relative motion:

$$\frac{d\mathbf{r}}{d\xi} = \alpha(\xi) t_c \mathbf{u}, \tag{12}$$

$$\frac{d\mathbf{u}}{d\xi} = \frac{\alpha(\xi) t_c}{m}[\mathbf{F}(\mathbf{r}) - \mathbf{F}(-\mathbf{r})], \tag{13}$$

where $\alpha(\xi) = 10^{\xi} \ln 10 \approx 2.30 \times 10^{\xi}$. Assuming that the xz plane is formed by the internuclear axis and the direction of motion of the molecular ion, the equations for the x and z components of the relative position and the relative velocity, which are suitable for a MD simulation over a long period of time, can be derived from Eqs. (12) and (13) as follows:

$$dx/d\xi = \alpha(\xi) t_c u_x,$$

$$dz/d\xi = \alpha(\xi) t_c u_z, \tag{14}$$

$$du_x/d\xi = \frac{\alpha(\xi) t_c}{m}[2F_x^C(x,z) + F_x^P(x,z) - F_x^P(-x,-z)],$$

$$du_z/d\xi = \frac{\alpha(\xi) t_c}{m}[2F_z^C(x,z) + F_z^P(x,z) - F_z^P(-x,-z)].$$

Equations (14) provide a self-consistent procedure to determine the dynamics of Coulomb explosion of a dicluster by using appropriate initial conditions for the relative separation $\mathbf{r}_0$, which can be expressed in the xz plane by $\mathbf{r}_0 = (r_0 \sin\theta_0, r_0 \cos\theta_0)$ with θ_0 being the initial azimuthal angle in the range from $-\pi/2$ to $\pi/2$, and for the initial relative velocity $\mathbf{u}_0$, which we take to be zero. In the following, we solve Eqs. (14) numerically for the case of a H_2^+ projectile, so that $Z_1 = 1$, $r_0 = 1.06 \times 10^{-8}$ cm, and $t_c \approx 1.47$ fs, while assuming that the initial angle is $\theta_0 = 60°$.

Figure 4 shows the influences of the variations of (a) the projectile velocity $v_p = v_T$, $2v_T$, and $3v_T$, (b) the plasma density $n_0 = 10^{21}$ cm^{-3}, 10^{22} cm^{-3}, and 10^{23} cm^{-3}, and (c) the electron temperature $T_e = 10$ eV, 10^2 eV, and 10^3 eV on the dependence of the logarithm of internuclear distance $\log_{10}(r/r_0)$ on the logarithm of penetration time $\xi = \log_{10}(t/t_c)$, during Coulomb explosions of H_2^+ with a standard set of parameters $v_p = v_T$, $n_0 = 10^{23}$ cm^{-3}, and $T_e = 10$ eV. It can be seen from Figs. 4(a)–4(c) that all cases are qualitatively very similar, with some minor quantitative differences, indicating that the Coulomb explosion proceeds faster for higher speeds, lower plasma densities, and higher temperatures. Considering that rather broad ranges of plasma densities and electron temperatures were used in Fig. 4, the qualitative similarity of the curves can be explained by the fact that in all cases the Debye length and the wavelength of the wake oscillations are so large that the initial stage of the explosion is practically completed under the action of bare Coulomb force, and the collective plasma effects only become important in the late stages, when the explosion has entered ballistic regime.

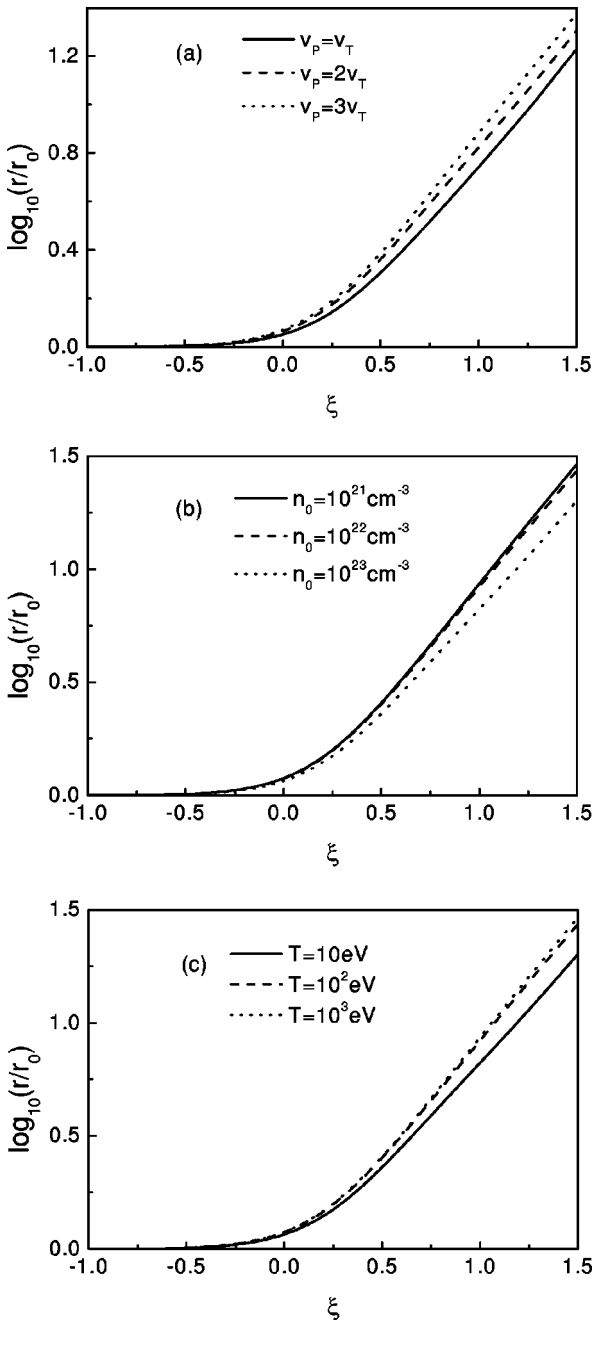

FIG. 4. Internuclear distance r as a function of the logarithm of the penetration time $\xi = \log_{10}(t/t_c)$ during the Coulomb explosion of a hydrogen molecular ion with the initial angle $\theta_0 = 60°$, moving through plasmas with (a) different velocities $v_p = v_T$, $2v_T$, and $3v_T$, and fixed plasma density $n_0 = 10^{23}$ cm^{-3} and electron temperature $T_e = 10$ eV; (b) different plasma densities $n_0 = 10^{21}$ cm^{-3}, 10^{22} cm^{-3}, and 10^{23} cm^{-3}, and fixed plasma temperature $T_e = 10$ eV and velocity $v_p = v_T$; (c) different electron temperatures $T_e = 10$ eV, 100 eV, and 1000 eV, and fixed plasma density $n_0 = 10^{23}$ cm^{-3} and velocity $v_p = v_T$.

Figures 5(a)–5(c) show the angle θ between the molecu-

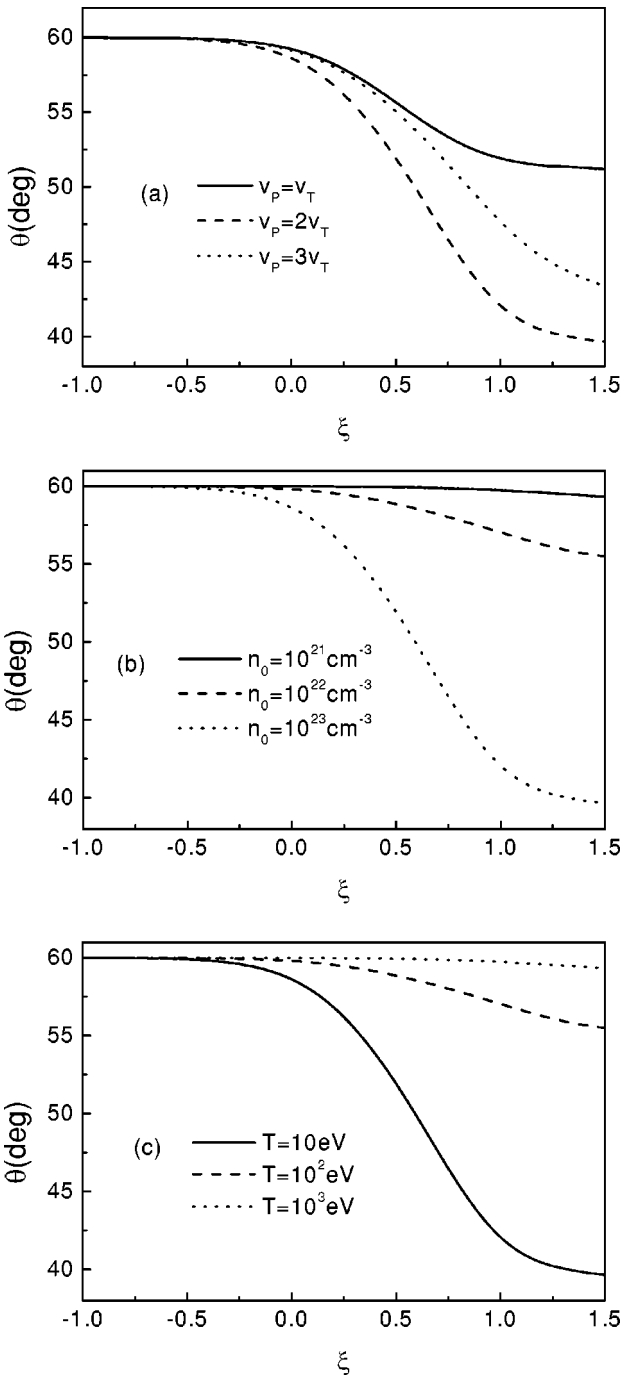

FIG. 5. The dependence of the angle θ between the molecular axis and the beam direction on the logarithm of the penetration time $\xi=\log_{10}(t/t_c)$ during the Coulomb explosion of a hydrogen molecular ion with the initial angle $\theta_0=60°$, moving through plasmas, with the same set of parameters as those used in Figs. 4(a)–4(c).

lar axis and the beam direction as a function of the logarithm of penetration time $\xi=\log_{10}(t/t_c)$ for the same set of parameters as in Figs. 4(a)–4(c). One can see from Fig. 5 that, due to asymmetry of the interaction potential, the molecular axis generally tends to align itself along the beam direction in the course of Coulomb explosion. However, in contrast to Fig. 4, here the influences of all three parameters v_p, n_0, and T_e on rotation of the molecular axis are surprisingly diverse in both the early and the ballistic stages of the explosion. It appears that, generally, tilting of the axis in the direction of motion is stronger in dense and cold plasmas, that is, for shorter Debye lengths.

IV. STOPPING POWER

From Eq. (10) one can obtain the expression for the stopping power of the molecular ion in the following form [24]:

$$S_{mol}=2S_{Z_1}(v_p)+S_v(x,z,v_p), \tag{15}$$

where $S_{Z_1}(v_p)=-F_s(v_p)$ is the stopping power of a single ion with charge Z_1, while $S_v(x,z,v_p)=-F_z^P(x,z,v_p)-F_z^P(-x,-z,v_p)$ is the so-called vicinage stopping power. The first term on the right-hand side of Eq. (15) gives the stopping power of two uncorrelated ions, while the second term introduces the interferences in molecular stopping due to spatial correlation among the constituent ions of the cluster. We note that, upon solving the equations for relative motion of ions during the Coulomb explosion, the components x and z of the interionic separation become functions of time t, and so does the vicinage stopping power $S_v(x,z,v_p)$.

Figures 6(a) and 6(b) show the stopping power $S_{Z_1}(v_p)$ for proton ($Z_1=1$) as a function of the projectile velocity for different plasma densities and for different electron temperatures, respectively. One can see from these figures that the stopping power S_{Z_1} increases with the plasma density and decreases with the electron temperature, while exhibiting a maximum for the velocity $v_p\approx v_T$.

Finally, in order to clarify the role of Coulomb explosions in the vicinage effect on the molecular energy loss, we show in Figs. 7(a)–7(c) the stopping power ratio $R=1+S_v(x,z,v_p)/2S_{Z_1}(v_p)$, as a function of the logarithm of the penetration time $\xi=\log_{10}(t/t_c)$, for a H_2^+ molecule moving at various speeds through plasmas with various densities and various electron temperatures, using the same set of parameters as those in Figs. 4(a)-4(c). One can see that, in the early stages of Coulomb explosion, when the two constituent ions are so close to each other that they act as if they were almost united into a single point-like projectile with the double charge, the molecular energy loss is significantly enhanced compared to the energy loss of two independent isotachic protons. Figures 7(a)–7(c) show that this enhancement is greater for, respectively, faster projectiles, lower plasma densities, and higher electron temperatures. On the other hand, for prolonged penetration times t, the stopping ratio R approaches 1, indicating that the two ions have moved away from each other in the course of Coulomb explosion to sufficiently large separations, so that they act as two completely independent, or uncorrelated, perturbers of the plasma. In order to better understand quantitative features of the results in Fig. 7, we mention that, in analogy to the analysis of molecular stopping in solids [24], one expects that the vicinage effect will give rise to enhanced energy losses when the internuclear separation r is smaller than the so-called adiabatic screening length v_p/ω_p. Moreover, based on the above discussion of Fig. 4, late stages of Coulomb explosion are

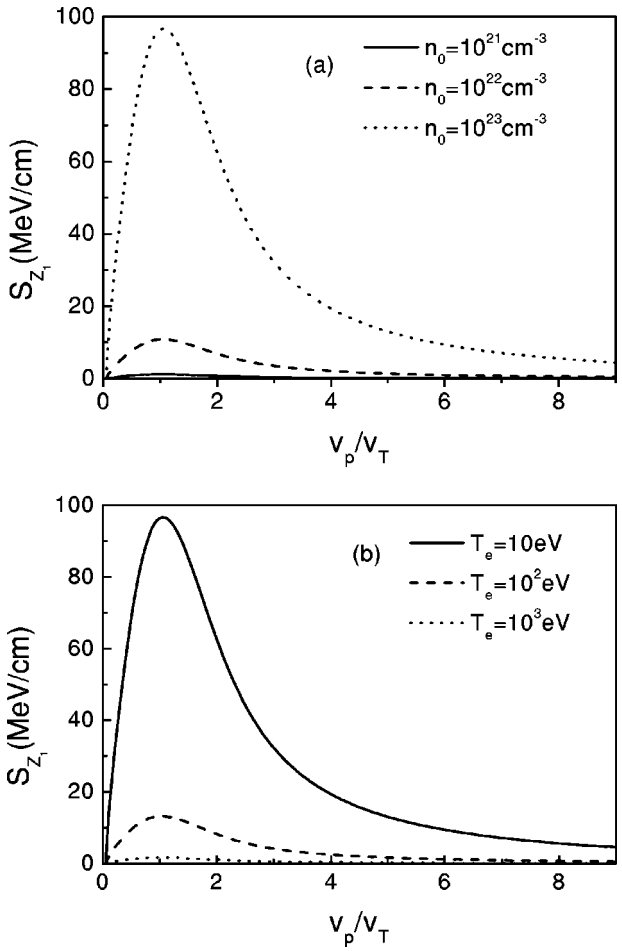

FIG. 6. Proton stopping power as a function of the velocity ratio v_p/v_T in plasmas with (a) different plasma densities $n_0 = 10^{21}$ cm^{-3}, 10^{22} cm^{-3}, and 10^{23} cm^{-3}, and fixed plasma temperature $T_e = 10$ eV; (b) different plasma temperatures $T_e = 10$ eV, 10^2 eV, and 10^3 eV, and fixed plasma density $n_0 = 10^{23}$ cm^{-3}.

characterized by the ballistic motion where $r \simeq r_0 t/t_c$. Therefore, one may estimate the time after which the vicinage effect on the energy loss diminishes to be of the order of $v_p t_c/(r_0 \omega_p)$, as can be seen in Fig. 7. We note that, depending on plasma parameters, this time scale may cover a broad range from femtoseconds to picoseconds.

V. SUMMARY

We have studied the interactions of a swift diatomic molecular ion with a classical plasma target using the linearized Vlasov-Poisson theory. Both the interaction potential and the corresponding force among the two constituent ions have been divided into bare Coulomb part and the polarization part which describes an oscillatory, long-range asymmetric interaction. Numerical results show that the projectile velocity is an important parameter affecting the interaction among the ions, in such a manner that both the amplitude and the range of oscillations in the polarization potential increase with increasing velocity.

Furthermore, using the results for the total interaction force, we have solved numerically the equations of motion for the two ions in order to reveal the effects of the projectile velocity and the plasma parameters on the Coulomb explosion dynamics. It has been found that, due to the wake effects, the molecular axis generally tends to align itself along the beam direction with increasing penetration time.

Finally, using the results for the relative motion of the two

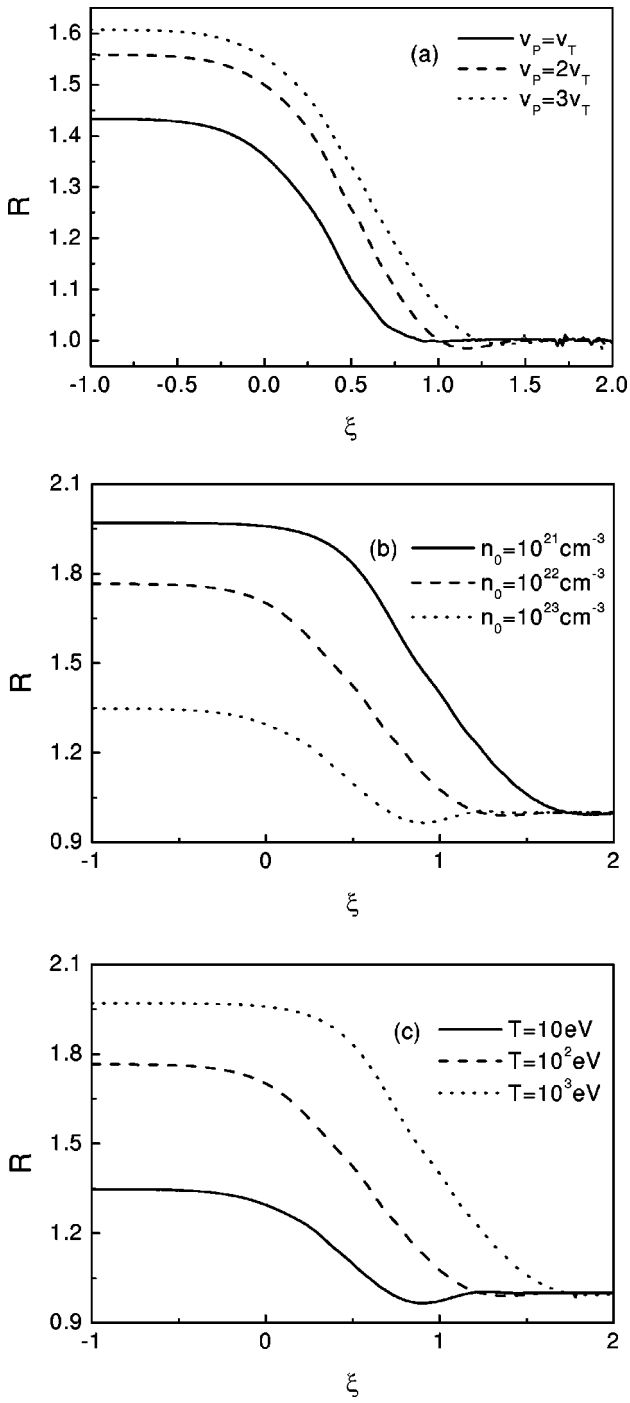

FIG. 7. Stopping power ratio R as a function of the logarithm of the penetration time $\xi = \log_{10}(t/t_c)$ during the Coulomb explosion of a hydrogen molecular ion with the initial angle $\theta_0 = 60°$, moving through plasmas, with the same set of parameters as those used in Figs. 4(a)–4(c).

constituent ions during the Coulomb explosion, we have found that the molecular stopping power is increased in the early stages of Coulomb explosion, due to constructive interferences in the vicinage effect, but decreases with increasing penetration time as the constituent ions fly apart to distances large compared to the adiabatic screening length. It was shown that the vicinage effect on the molecular energy loss is strongly influenced by variations in the projectile speed and in the plasma parameters.

The results obtained in the present work may be helpful in further studies aiming at controlling the rate of energy deposition of molecular and cluster ions in plasma targets for ICF experiments. In particular, it appears that the Coulomb explosion dynamics introduces the time and the length scales which may be useful in designing optimal regimes for ion-cluster penetration through classical plasmas, which take advantage of enhanced energy losses compared to the isolated ions.

ACKNOWLEDGMENTS

This work was jointly supported by the National Natural Science Foundation of China (Grant No. 10275009) and the Grant for Striding-Century Excellent Scholar of Ministry of Education State of China. Z.L.M. acknowledges the support by the Natural Sciences and Engineering Research Council of Canada.

[1] R.C. Arnold and J. Meyer-ter-Vehn, Rep. Prog. Phys. **50**, 559 (1987).
[2] N.R. Arista, R.O.M. Galvão, and L.C.M. Miranda, J. Phys. Soc. Jpn. **59**, 544 (1990).
[3] O. Boine-Frankenheim and J. D'Avanzo, Phys. Plasmas **3**, 792 (1996).
[4] H.B. Nersisyan, M. Walter, and G. Zwicknagel, Phys. Rev. E **61**, 7022 (2000).
[5] J. D'Avanzo, I. Hofmann, and M. Lontano, Phys. Plasmas **3**, 3885 (1996).
[6] H.B. Nersisyan, G. Zwicknagel, and C. Toepffer, Phys. Rev. E **67**, 026411 (2003).
[7] O. Boine-Frankenheim, Phys. Plasmas **3**, 1585 (1996).
[8] G. Zwicknagel, Nucl. Instrum. Methods Phys. Res. B **197**, 22 (2002).
[9] J. D'Avanzo, M. Lontano, and P.F. Bortignon, Phys. Rev. A **45**, 6126 (1992).
[10] J. D'Avanzo, M. Lontano, and P.F. Bortignon, Phys. Rev. E **47**, 3574 (1993).
[11] J. D'Avanzo, M. Lontano, E. Tome, and P.F. Bortignon, Phys. Rev. E **52**, 919 (1995).
[12] C. Deutsch and P. Fromy, Phys. Rev. E **51**, 632 (1995).
[13] G. Zwicknagel and C. Deutsch, Nucl. Instrum. Methods Phys. Res. A **415**, 599 (1998).
[14] G. Zwicknagel and C. Deutsch, Phys. Rev. E **56**, 970 (1997).
[15] H.B. Nersisyan and C. Deutsch, Phys. Lett. A **246**, 325 (1998).
[16] H.B. Nersisyan and E.A. Akopyan, Phys. Lett. A **258**, 323 (1999).
[17] M. Lontano and F. Raimondi, Phys. Rev. E **51**, R2755 (1995).
[18] Y.-N. Wang, H.-T. Qiu, and Z.L. Mišković, Phys. Rev. Lett. **85**, 1448 (2000).
[19] G.Q. Wang, Y.H. Song, Y.N. Wang, and Z.L. Mišković, Phys. Rev. A **66**, 042901 (2002).
[20] M.M. Jakas and N.E. Capuj, Phys. Rev. A **54**, 5031 (1996).
[21] Z.L. Mišković, S.G. Davison, F.O. Goodman, W.-K. Liu, and Y.N. Wang, Phys. Rev. A **63**, 022901 (2001).
[22] H.W. Li, Y.N. Wang, and Z.L. Mišković, Nucl. Instrum. Methods Phys. Res. B **193**, 204 (2002).
[23] A. Bret and C. Deutsch, Fusion Eng. Des. **32-33**, 517 (1996).
[24] N. Arista, Nucl. Instrum. Methods Phys. Res. B **164-165**, 108 (2000).